Knock Characteristics in Liquefied Petroleum Gas (LPG)−Dimethyl Ether (DME) and Gasoline−DME Homogeneous Charge Compression Ignition Engines

Kitae Yeom and Choongsik Bae*

Department of Mechanical Engineering, Korea Advanced Institute of Science and Technology (KAIST), 373-1, Guseong-dong, Yuseong-gu, Taejon 305-701, Republic of Korea

Received October 6, 2008. Revised Manuscript Received January 25, 2009

The knock characteristics in an engine were investigated under homogeneous charge compression ignition (HCCI) operation. Liquefied petroleum gas (LPG) and gasoline were used as fuels and injected at the intake port using port fuel injection equipment. Dimethyl ether (DME) was used as an ignition promoter and was injected directly into the cylinder during the intake stroke. Different intake valve timings and fuel injection amounts were tested to verify the knock characteristics of the HCCI engine. The LPG is more suitable for high-load operation of HCCI than gasoline because of its high latent heat of vaporization and octane number. The knock intensity of LPG−DME combination was lower than that of gasoline−DME, because of the lower self-ignitability and the higher latent heat of vaporization of the total injected fuel. The ringing intensity (RI) increased as the intake valve open (IVO) timing was advanced. This is attributed to higher volumetric efficiency and residual gas, which promotes combustion. The knock intensity can be predicted by measuring and calculating the crank angle degree of 50% mass fraction burned. Carbon monoxide and hydrocarbon emissions were minimized at high ringing intensity conditions. The shortest burn duration under 0.5 MW/m^2 of RI was effective in achieving low hydrocarbon and carbon monoxide emissions.

1. Introduction

The homogeneous charge compression ignition (HCCI) engine is regarded as one of the future engine technologies because of its lower nitric oxide (NO_x) emissions and better fuel economy characteristics.[1] The nature of the HCCI engine is a combination of spark-ignition (SI) and compression-ignition (CI) engines in its mixture preparation and ignition process, respectively. The HCCI engine breathes premixed charge and ignites it by a chemical reaction, which is initiated by compression heat and pressure.[1] This chemical reaction occurs during an extremely short duration at every single point of the combustion chamber almost simultaneously.[2] A higher compression ratio or larger amount of residual gas, which provides more heat, is needed to ignite the charge with high-octane-number fuels, such as gasoline and liquefied petroleum gas (LPG).[3,4] A high-cetane-number fuel, such as diesel and dimethyl ether (DME), can promote the ignition process. However, these ignition promotion methods also accelerate the speed of combustion.[5,6] Fast and early combustion leads to not only a higher combustion pressure and a higher rate of pressure rise but also a higher engine noise and a possibility of damage.[1]

The combustion of HCCI is very similar to the knock phenomenon in SI engine operation because of its almost simultaneous self-ignition.[7] SI knock is the auto-ignition of the end gas ahead of the normal flame front.[8,9] In the case of SI engines, the spark timing for the best torque is limited by knock.[9] Similarly, the HCCI-engine-operating range is limited by high combustion pressure, high rate of pressure rise, and heavy knock.[10,11]

An SI knock analysis based on cylinder pressure can be performed quantitatively, using the methods based on the following items:[7] (1) the evaluation of a single pressure value, (2) pressure derivatives, (3) frequency domain manipulations, and (4) heat release analysis.

* To whom correspondence should be addressed. Fax: 82-42-869-5044. E-mail: csbae@kaist.ac.kr.

(1) Zhao, F.; Asmus, T.; Assanis, D.; Dec, J.; Eng, J.; Najt, P. *Homogeneous Charge Compression Ignition (HCCI) Engines: Key Research and Development Issues*; Society of Automotive Engineers (SAE): Warrendale, PA, 2003; PT-94.

(2) Kaiser, E.; Yang, J.; Culp, T.; Xu, N.; Maricq, M. Homogeneous charge compression ignition engine-out emissions−Does flame propagation occur in homogeneous charge compression ignition. *Int. J. Engine Res.* **2002**, *3* (4), 185–196.

(3) Yap, D.; Karlovsky, J.; Megaritis, A.; Wyszynski, M.; Xu, H. An investigation into propane homogeneous charge compression ignition engine operation with residual gas trapping. *Fuel* **2005**, *84* (18), 2372–2379.

(4) Yap, D.; Megaritis, A.; Wyszynski, M. An investigation into bioethanol homogeneous charge compression ignition (HCCI) engine operation with residual gas trapping. *Energy Fuels* **2004**, *18*, 1315–1323.

(5) Xingcai, L.; Yuchun, H.; Libin, J.; Linlin, Z.; Zhen, H. Heat release analysis on combustion and parametric study on emissions of HCCI engines fueled with 2-propanol/*n*-heptane blend fuels. *Energy Fuels* **2006**, *20*, 1870–1878.

(6) Kim, D.; Kim, M.; Lee, C. Effect of premixed gasoline fuel on the combustion characteristics of compression ignition engine. *Energy Fuels* **2004**, *18*, 1213–1219.

(7) Millo, F.; Ferraro, V. Knock in SI engines: A comparison between different techniques for detection and control. *SAE Trans.* **1998**, *107* (4), 1090–1111, SAE 2477.

(8) Abu-Qudais, M. Exhaust gas temperature for knock detection and control in spark ignition engine. *Energy Convers. Manage.* **1996**, *37* (9), 1383–1392.

(9) Seref, S. Prediction of knock limited operating conditions of a natural gas engine. *Energy Convers. Manage.* **2005**, *46* (1), 121–138.

(10) Griffiths, J.; MacNamara, J.; Sheppard, C.; Turton, D.; Whitaker, B. The relationship of knock during controlled autoignition to temperature inhomogeneities and fuel reactivity. *Fuel* **2002**, *81* (17), 2219–2225.

(11) Yeom, K.; Bae, C. Gasoline−dimethyl ether homogeneous charge compression ignition engine. *Energy Fuels* **2007**, *21* (4), 1942–1949.

10.1021/ef800846u CCC: $40.75
Published on Web 03/09/2009

The knock intensity could be represented by the peak combustion pressure. However, the peak combustion pressure can be changed according to the operating conditions of the test engine.[7] To overcome this defect, the rate of pressure rise was used. In this case, the minimum value of the third derivative of pressure was used as an indicator of knock intensity for minimum disturbance.[12] A method using the window energy at the frequency domain of knock has also been reported.[13] Three indices of knock intensity on the basis of a number of band-pass-filtered cylinder pressure signals were used, such as integral of modulus of pressure gradient (IMPG), integral of modulus of pressure oscillation (IMPO), and maximum amplitude of pressure oscillation (MAPO).[14−16] A new method that can represent the knock intensity of HCCI combustion is needed because of its different combustion nature in HCCI engines, and therefore, the ringing intensity (RI) was introduced.[17] The RI indicates the wave energy of pressure oscillation because of knock.[17] The RI is shown as below

$$\mathrm{RI} = \frac{1}{2\gamma}\frac{\sqrt{\gamma RT}}{P}\frac{1}{N}\sum_{1}^{N}\left[0.05\left(\frac{\partial p}{\partial t}\right)_{\max}\right]^2 \quad (1)$$

where γ is the specific heat ratio, P is the cylinder combustion pressure, R is the universal gas constant, T is the temperature, N is the number of cycles, and $(\partial p/\partial t)_{\max}$ is the maximum pressure rise.

In this paper, the knock intensity of LPG and gasoline HCCI at different valve timing and DME direct injection in an engine was examined as a series work of gasoline−DME HCCI combustion analysis.[18] The limits in the operating range of the test engine are defined by knock analysis and expanded by combustion phase control, using variable valve timing (VVT). The effects of LPG, residual gas, and volumetric efficiency were also investigated to find ways of widening the operating range.

2. Experimental Section

2.1. Experimental Apparatus. The specifications of the engine are given in Table 1. The base engine is a four-cylinder SI engine and has a double overhead camshaft (DOHC) equipped with VVT. A cylinder was modified for HCCI combustion with a DME direct-injection system on the cylinder head. An engine control unit (ECU) (Motec Co., M4) was employed to precisely control DME quantity and injection timing. A second ECU (ETAS Co.) was used to control the quantity and timing of port fuel injection and intake valve timing. The resolution of the engine control system was 0.001 CAD.

Figure 1 shows a schematic diagram of the experimental setup. The engine speed and load were controlled with an alternating current (AC) dynamometer. A liquid-phase injection system was used for LPG injection into the intake manifold. This system can improve the volumetric efficiency via liquid-phase injection and lower the intake air temperature, owing to the heat absorption during LPG vaporization at the intake port. Additionally, reduced engine emissions can be achieved with precise mixture control, as in gasoline SI engines. A slit injector (Denso Co.) was used to inject DME directly into the cylinder at a constant supply pressure of 5 MPa, using pressurized nitrogen gas. The DME injector was located at the spark plug hole of the research engine. A lubricity enhancer (Infineum, R655) of 500 ppm was added to the DME to avoid damage to the fuel injection system. The in-cylinder pressure was measured using a piezoelectric pressure transducer (Kistler, 6052b). A short time drift of the cylinder pressure sensor because of thermal shock is under ±0.05 MPa. The sensitivity change of the pressure transducer is less than ±0.5% of measured value. The intake and exhaust manifold pressures were measured by two piezo-resistive pressure transducers (Kistler, 4045A5), while the intake and exhaust temperatures were measured with two K-type thermocouples. A wide-band lambda meter (ETAS, LA4) was installed for the measurement of the relative air/fuel ratio. Exhaust gases were analyzed with a gas analyzer (Horiba, Mexa 1500D) to measure the HC, NO_x, CO, and CO_2 emissions. The accuracy of the exhaust gas measuring system is ±1.0% of full scale. Two data acquisition systems (IOtech, Wavebook 512H) were employed to acquire all engine combustion and exhaust gas data. A/D resolution, speed, and accuracy are 12 bit, 1 MHz, and ±0.025% of full scale, respectively. The data including mass air flow rate and exhaust gases (HC, CO, CO_2, and NO_x) were acquired at 1 kHz sampling rate.

Table 1. Engine Specifications

bore (mm)		82
stroke (mm)		93.5
compression ratio		13
displacement (cc)		494
intake/exhaust valve opening duration (CAD)		228/228
intake/exhaust valve lift (mm)		8.5/8.4
valve timing (CAD)	intake valve open (ATDC)	from −29 to 11
	intake valve close (ABDC)	from 59 to 19
	exhaust valve open (BBDC)	42
	exhaust valve close (ATDC)	6
DME injection pressure (MPa)		5
LPG injection pressure (MPa)		1.5
gasoline injection pressure (MPa)		0.3
DME injector		slit injector
LPG injector		single-hole port fuel injector
gasoline injector		multihole port fuel injector

The VVT system can vary the open and close timing of the intake valve. The intake valve open (IVO) timing was varied over a range of 29 crank angle degrees (CADs) before top dead center (BTDC) to 11 CADs after top dead center (ATDC), while the valve duration was fixed at 228 CADs. Generally, volumetric efficiency and residual gas increase as IVO timing is advanced at low engine speeds. The start of HCCI combustion is affected by surrounding conditions, such as pressure, fuel distribution, and temperature of the mixture during compression stroke.[1] The temperature and pressure of charge are increased and reach the auto-ignition point earlier, when the volumetric efficiency and residual gas fraction are higher, because of the combustion enhancement.

2.2. Experimental Conditions. Table 2 shows the main experimental conditions used in this study. The engine speed was fixed at 1000 rpm, and the IVO timing and relative air/fuel ratio were varied from −29 to 11 CADs ATDC and from 2.91 to 2.12, relatively. The air/fuel ratio, A/F, is defined as the ratio $\dot{m}_a/\dot{m}_f$.[19] The relative air/fuel ratio, λ, is defined as the ratio of the actual air/fuel ratio to the stoichiometric air/fuel ratio; $(A/F)_{actual}/(A/F)_{stoichiometric}$.[19] To define the λ of each fuel, the total mass of fresh air and the injection quantity of each fuel were used.

(12) Checkle, M.; Dale, J. Computerized knock detection from engine pressure records. SAE Tech. Pap. 860028, 1986.

(13) Brunt, M.; Pond, C.; Biundo, J. Gasoline engine knock analysis using cylinder pressure data. *SAE Trans.* **1998**, *106* (3), 1399–1412, SAE 0896.

(14) Brecq, G.; Ramesh, A.; Tazerout, M. A new indicator for knock detection in gas SI engines. *Int. J. Therm. Sci.* **2003**, *42* (5), 523–532.

(15) Ramesh, A.; Brecq, G.; Tazerout, M.; Le Corre, O. Knock rating of gaseous fuels in a single cylinder spark ignition engine. *Fuel* **2004**, *83* (3), 327–336.

(16) Hudson, C.; Gao, X.; Stone, R. Knock measurement for fuel evaluation in spark ignition engines. *Fuel* **2001**, *80* (3), 395–407.

(17) Eng, J. Characterization of pressure waves in HCCI combustion. SAE Tech. Pap. 2002-01-2859, 2002.

(18) Yeom, K.; Jang, J.; Bae, C. Homogeneous charge compression ignition of LPG and gasoline using variable valve timing in an engine. *Fuel* **2007**, *86* (4), 494–503.

(19) Heywood, J. *Internal Combustion Engine Fundamentals*; McGraw-Hill: New York, 1988.

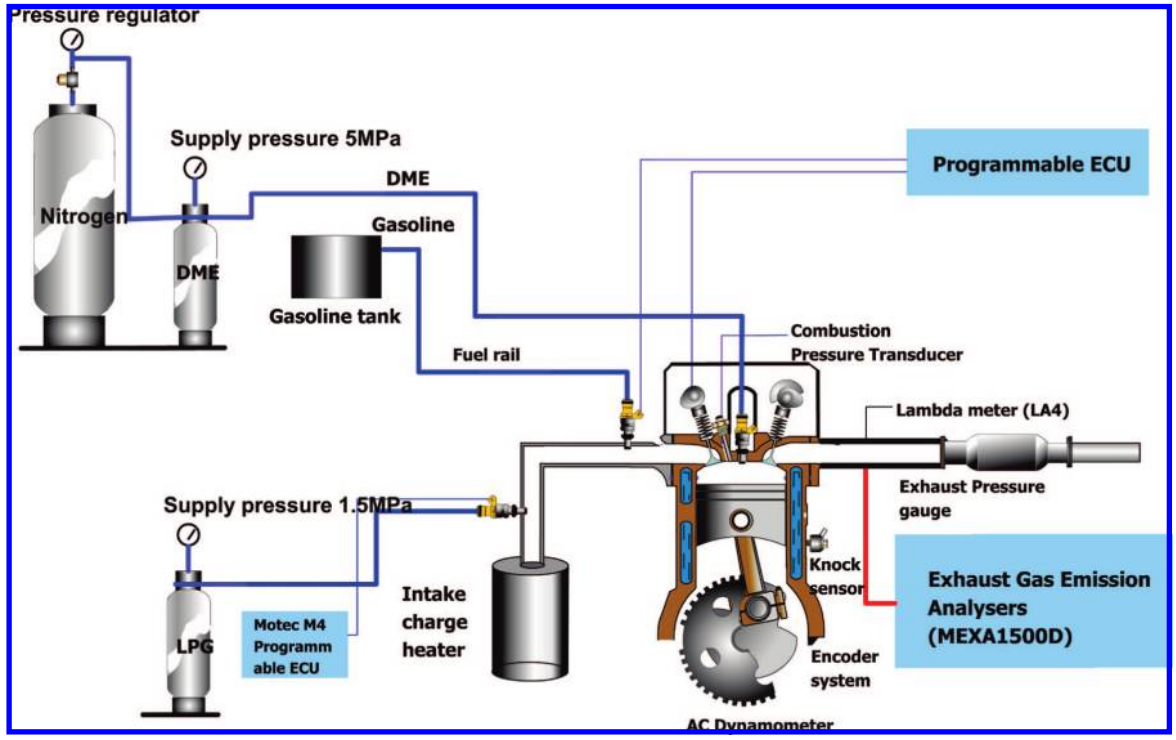

Figure 1. Schematic diagram of the experimental apparatus.

Table 2. Experimental Conditions

engine speed (rpm)	1000
intake valve open timing (CAD)	−29, −19, −9, 1, and 11
DME injection timing (CAD)	110
LPG and gasoline injection timing (CAD)	470
λ_{total}	2.12, 2.41, 2.57, 2.77, and 2.91
λ_{DME}	3.70
λ_{LPG} and $\lambda_{gasoline}$	4.96, 6.91, 8.42, 11.02, and 13.63
intake charge temperature (°C)	30
coolant/oil temperature (°C)	80/80

λ_{total} is defined as a relative air/fuel ratio of the total mixture containing LPG or gasoline and DME, shown in eq 2, which was derived from a chemical oxidation formula of different λ_{total} conditions.

$$\lambda_{total} = \frac{\lambda_{LPG}\lambda_{DME}}{\lambda_{LPG} + \lambda_{DME}}, \quad \lambda_{total} = \frac{\lambda_{gasoline}\lambda_{DME}}{\lambda_{gasoline} + \lambda_{DME}} \qquad (2)$$

From the previous research, the importance of λ_{DME} on the start of combustion was unveiled. In the case of λ_{DME} being lower than 3 or higher than 4, there was too loud of an engine noise or no combustion. Because of this, λ_{DME} was fixed at 3.7 for the varied IVO and λ_{total} was varied from 2.12 to 2.91. The injector locations for the LPG and gasoline injection were 30 and 10 cm upstream from the intake valve, respectively. The engine was run at 1000 rpm for various intake valve timings and λ. The IVO timing was varied from −29 CADs ATDC to 11 CADs ATDC. The volumetric efficiency was 80, 79.5, and 77.2% at the IVO timing of −29, −19, and −9 CADs ATDC, respectively. Furthermore, the volumetric efficiency dropped rapidly at 1 CAD ATDC and 11 CADs ATDC of IVO, with values of 70.8 and 66.2%, respectively. Figure 2 shows the intake valve timing and the DME injection timing.

The mass flow rate of intake charge was measured using a laminar flow meter (Meriam Co., 50MC2-2S). The proportions of propane and butane in the LPG used in this study were 60 and 40%, respectively. The DME injection timing was fixed at 110 CADs ATDC for the formation of a homogeneous mixture. Gasoline and LPG were injected into the intake manifold at 470 CADs ATDC.

Table 3 shows the fuel properties used in this study.

2.3. In-Cylinder Pressure Measurements and Analysis. The piezoelectric pressure transducer for in-cylinder pressure measurement was flush-mounted inside the cylinder head to reduce pipe oscillation effects.[13]

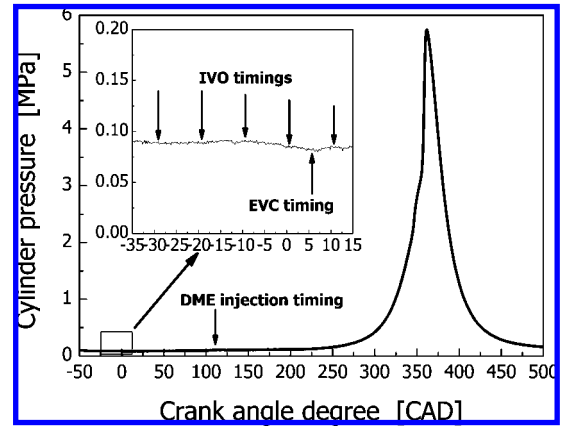

Figure 2. Intake valve open (IVO), exhaust valve close (EVC), and DME injection timing.

Table 3. Fuel Properties

	LPG	DME	gasoline
chemical formula	$C_3H_8 + C_4H_{10}$	CH_3OCH_3	
flammable temperature (K)	750−810	500	730−750
low heating value (MJ/kg)	46.09	44.00	28.40
stoichiometric air/fuel ratio	15.6	8.9	14.7
latent heat of vaporization (kJ/kg)	370	460	306
octane number	107		93
cetane number		55	

To analyze the pressure data precisely, a high-precision rotary encoder (2048 pulses/revolution) was used for engine control and data acquisition. The typical pressure oscillation frequency of knock is approximately 5 kHz. The pressure data were acquired at every rotary encoder. The indicated mean effective pressure (IMEP) and heat release rate were calculated from the cylinder pressure values.[19]

(20) Sjoberg, M.; Dec, J. Effects of engine speed, fueling rate, and combustion phasing on the thermal stratification required to limit HCCI knock intensity. *SAE Trans.* **2005**, *114* (3), 1472–1486, SAE 2125.

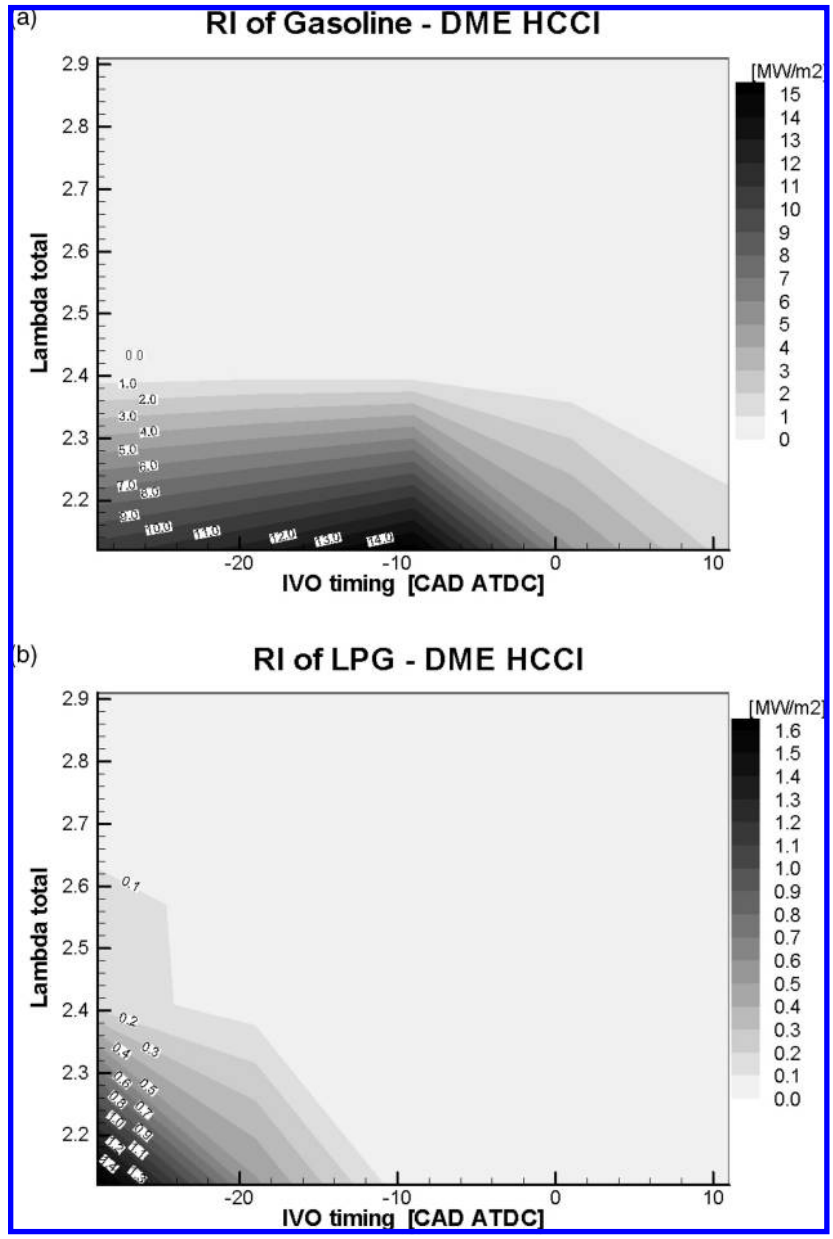

Figure 3. RI of HCCI combustion with respect to λ_{total} and IVO timing at 1000 rpm: (a) gasoline−DME HCCI and (b) LPG−DME HCCI.

The difference in lower heating values (LHVs) of LPG and gasoline used in this study was less than 0.3%.

3. Results

3.1. Ringing Intensity Analysis. Figure 3 shows the ringing intensity (RI) in HCCI combustion with gasoline and LPG, respectively, with respect to λ_{total} and intake valve open timing at 1000 rpm. The horizontal axis represents the intake valve open timing, and the vertical axis represents λ_{total}. It should be noted that the RI scales of two graphs are different, where the gasoline−DME case has almost a 10 times bigger scale than LPG−DME. The allowable operating range based on audible knock sounds is regarded as under 5 MW/m^2 of RI, which limits the high load operating range.[20,21] In the case of gasoline−DME HCCI, the RI was over 5 MW/m^2 when λ_{total} was lower than 2.3 and the IVO timing was more advanced than −10 CADs. The RI increased as the IVO timing was advanced. This is attributed to increased volumetric efficiency and residual gas, which promote combustion.

The fresh charge temperature reached 800−1000 K easily at the compression stroke because of the increased volumetric efficiency. The residual gas increased as the valve overlap period was increased.[22] The valve overlap period is the duration, while the intake and exhaust valves are open simultaneously. The exhaust gas is trapped by the pressure difference between the intake and exhaust ports. The heat transfer from hot residual gas to the fresh charge increased, which promotes ignition.[23] The charge temperature reaches a low-temperature reaction (LTR) temperature, which is 600−900 K,[1] more rapidly when the residual gas is more trapped in the combustion chamber. In the case of LPG−DME, the RI did not exceed 5 MW/m^2 at

(21) Helmantel, A.; Denbratt, I. HCCI operation of a passenger car DI diesel engine with an adjustable valve train. SAE Tech. Pap. 2006-01-0029, 2006.

(22) Cavina, N.; Ponti, F.; Siviero, C.; Suglia, R. Residual gas fraction estimation for model-based variable valve timing and spark advance control. ASME Internal Combustion Engine Division, 2004; ICEF2004-0956, pp 457−466.

(23) Caton, A.; Simon, J.; Gerdes, C.; Edwards, F. Residual-effected homogeneous charge compression ignition at a low compression ratio using exhaust reinduction. *Int. J. Engine Res.* **2003**, *4* (3), 163–178.

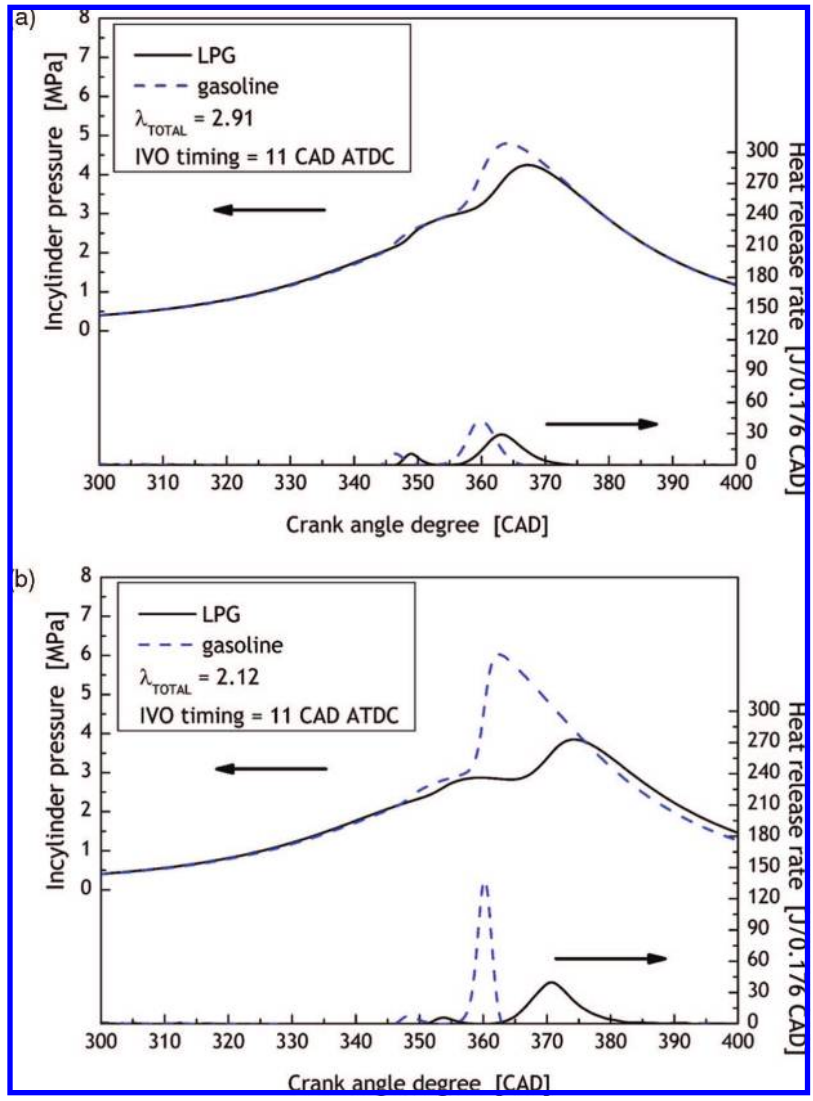

Figure 4. Combustion pressure and heat release rate of HCCI combustion with respect to λ_{total} at 1000 rpm: (a) $\lambda_{total} = 2.91$ and (b) $\lambda_{total} = 2.12$.

any operating condition. The reason for the lower RI value of LPG−DME HCCI compared to gasoline−DME HCCI is the late combustion, which is due to the lower self-ignitability of injected fuel and the larger latent heat of vaporization of total injected fuel. HCCI engine combustion is influenced by the chemical formation, temperature, and pressure of the air/fuel mixture.[1] The octane number of LPG (RON 107) used in this study is higher than gasoline (RON 93).[19] Because of the low octane number, the gasoline−DME mixture has better ignitability than the LPG−DME mixture. The self-ignitability of total injected fuel decreased as λ_{total} decreased, because of lower λ_{LPG} and fixed λ_{DME}. The decrease in self-ignitability of total fuel is one cause of late combustion.[1] Another cause is a lower intake temperature because of the latent heat of vaporization of LPG. The latent heat of vaporization of LPG used in this study is 370 kJ/kg, and that of gasoline is 306 kJ/kg. Because of the latent heat of vaporization, the temperature of the LPG/air mixture before the start of combustion was lower than that of the gasoline/air mixture by 2 K. These two reasons are proven by Figure 4, which shows the in-cylinder pressure and heat release rate of LPG−DME and gasoline−DME combustion. LPG−DME combustion started later than gasoline−DME combustion at the same operating conditions, and lower λ_{total} conditions show later combustion than higher λ_{total} conditions. In the case of the LPG−DME HCCI engine, the temperature of the air/fuel mixture is inversely proportional to the injection quantity of LPG. The octane number and temperature difference account for the difference in the start of combustion.

3.2. Combustion Characteristics and Ringing Intensity. Figure 5 shows the effect of knock resulting from early combustion on the IMEP. This figure shows that λ_{total} is the major parameter of the IMEP in the case of gasoline−DME HCCI. It is also noted that the two graphs have different scales because gasoline−DME has a higher level. There is an optimum amount of injected gasoline for attaining an optimal IMEP, corresponding to an approximate λ_{total} value of 2.4. When λ_{total} is lower than 2.4, the RI increases as IMEP drops rapidly. However, in the case of LPG−DME HCCI, the critical IMEP decrease was not observed. Higher volumetric efficiency and residual gas lead to early combustion, as explained. The RI, considered together with the IMEP, was more useful for the analysis of engine knock characteristics compared to the audible knock sounds. According to Figure 6, it was found that the IMEP was significantly affected by the RI value. The IMEP of the gasoline−DME and LPG−DME HCCI engines was decreased when the RI value was over 0.5 MW/m^2. This fact indicates that the high engine load should be limited to a certain range where the RI value is less than 0.5 MW/m^2.

Figures 7 and 8 show the maximum combustion pressure (P_{max}) to identify the relationship between the RI and P_{max}.

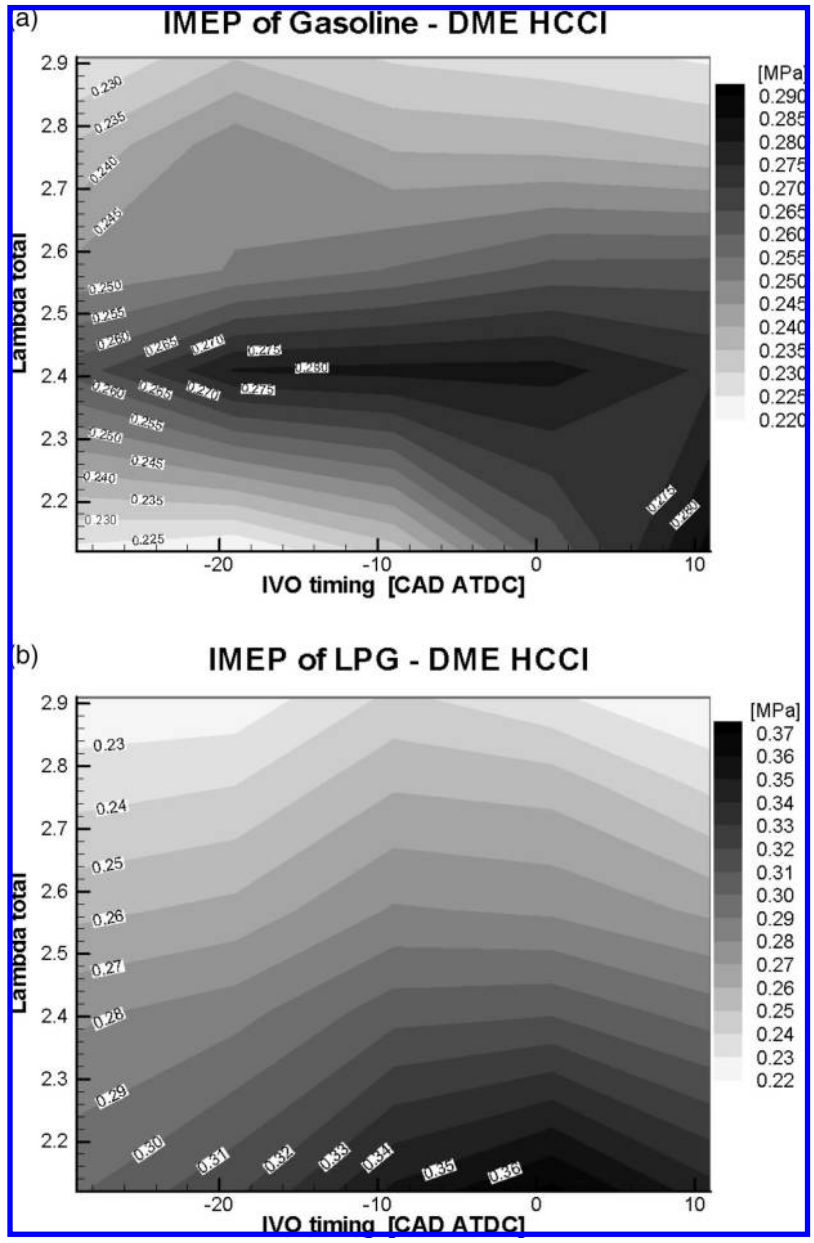

Figure 5. IMEP of HCCI combustion with respect to λ_{total} and IVO timing at 1000 rpm: (a) gasoline−DME HCCI and (b) LPG−DME HCCI.

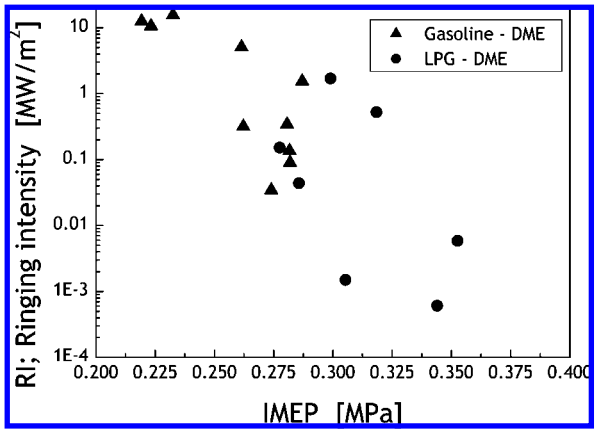

Figure 6. Ringing intensity with respect to IMEP (operating conditions, where λ_{total} is lower than 2.4, were shown).

Figure 8 shows the operating points with the IVO timing earlier than −9 CADs. According to Figures 3 and 5, higher than 0.5 MW/m^2 of RI and lower than 0.27 MPa of IMEP show the operating conditions for which P_{max} was over 6.6 MPa. This fact shows that most RI values higher than 0.5 MW/m^2 result from an overpressure rise higher than 6.6 MPa because of early combustion.

3.3. Ringing Intensity Estimation. The RI with respect to the crank angle degree at 50% mass fraction burned (CA50) of gasoline−DME and LPG−DME HCCI engines is shown in Figure 9. The RI was increased as the CA50 was advanced. The increase in the rate of the RI was reduced as λ_{total} increased. This is attributed to the reduction in the supplied LHV of the fuel. The RI that gradually increased apparently, because the CA50 was more advanced than that at 361 CADs. This graph shows that the combustion timing is another major factor of increased RI. The combustion phase control is needed to retard the CA50 and to reduce the RI at high RI operating conditions. This trend shows that the fuel type had no effect on the RI and CA50. The RI according to CA50 could be fit well to a

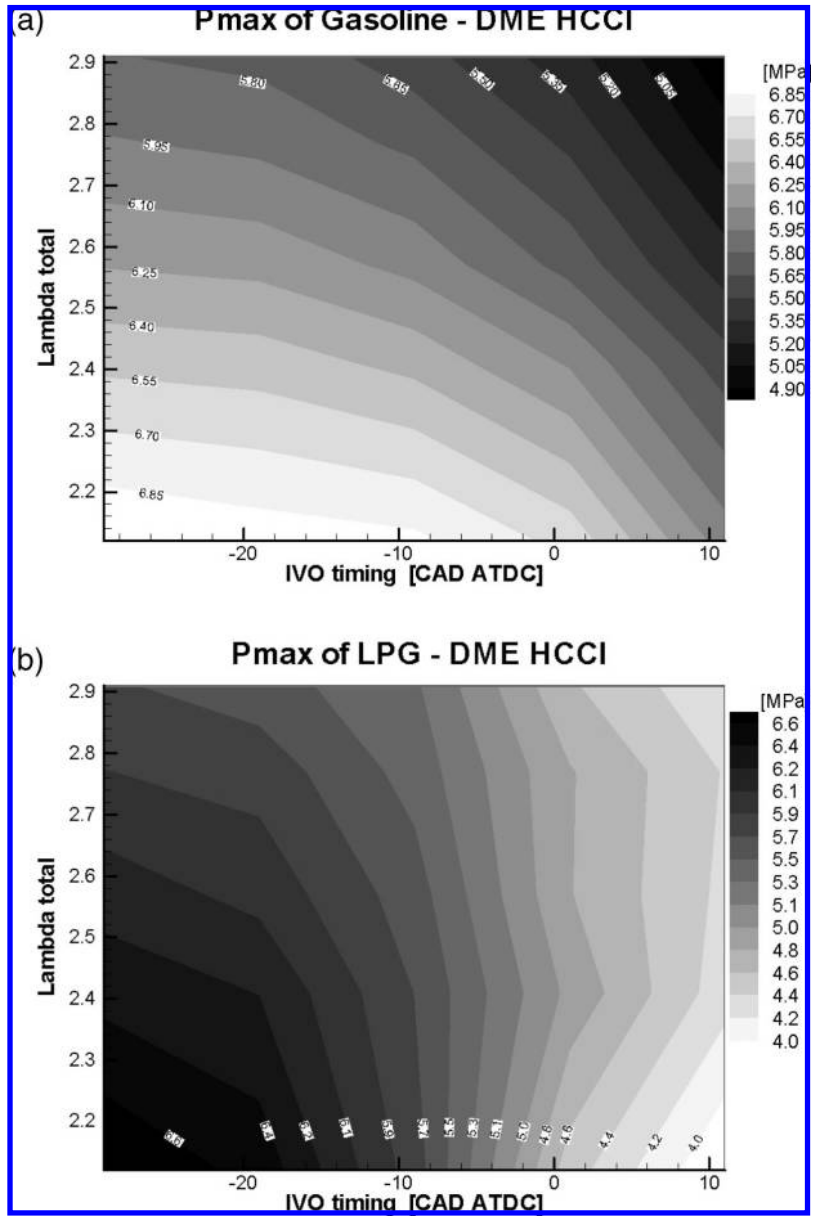

Figure 7. P_{max} of HCCI combustion with respect to λ_{total} and IVO timing at 1000 rpm: (a) gasoline−DME HCCI and (b) LPG−DME HCCI.

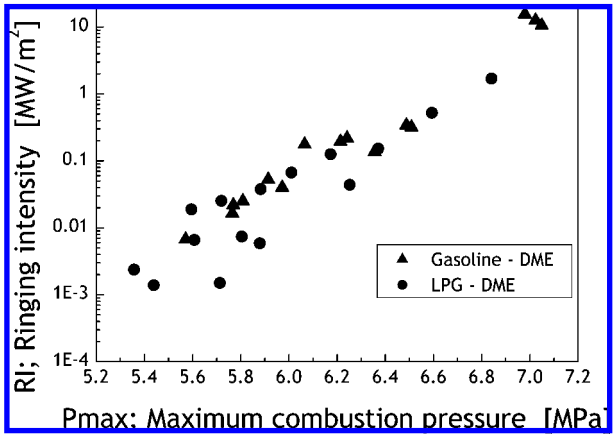

Figure 8. Ringing intensity with respect to P_{max} (for the operating conditions with IVO timings earlier than −9 CADs).

polynomial formulation, with a correlation coefficient R^2 over 0.95. Thus, the RI can be estimated by the CA50 or the P_{max}.

3.4. Exhaust Emissions. Figure 10 shows the ratio of carbon monoxide (CO) over carbon dioxide (CO_2) and hydrocarbon (HC) over all carbon contained in the exhaust emissions (CO, CO_2, and HC) with respect to RI of the gasoline−DME and LPG−DME HCCI engines at 1000 rpm. The mass fraction burned from 20 to 90%, with respect to RI, is shown in Figure 11.

The CO emissions of the HCCI engine are greater than those of SI or CI engines. This high CO emission is because of a lack of oxidation, which has a very close relationship with the combustion temperature during the expansion stroke. Consequently, CO emission is regarded as the index of incomplete combustion for HCCI engines.[1,2] The CO oxidation is influenced by the in-cylinder temperature.[24,25] The higher peak combustion pressure led to the higher combustion temperature. The CO/CO_2 ratio decreased as the RI increased. However, the CO/CO_2 ratio was approximately 0.17 at a negligible RI. Sjoberg and Dec reported that the high combustion temperature over 1500 K can help the CO oxidation process.[25] This implies that

(24) Bhave, A.; Kraft, M.; Montorsi, L.; Mauss, F. Sources of CO emissions in an HCCI engine: A numerical analysis. *Combust. Flame* **2006**, *144*, 634–637.

(25) Sjoberg, M.; Dec, J. An investigation into lowest acceptable combustion temperatures for hydrocarbon fuels in HCCI engines. *Proc. Combust. Inst.* **2005**, *30*, 2719–2726.

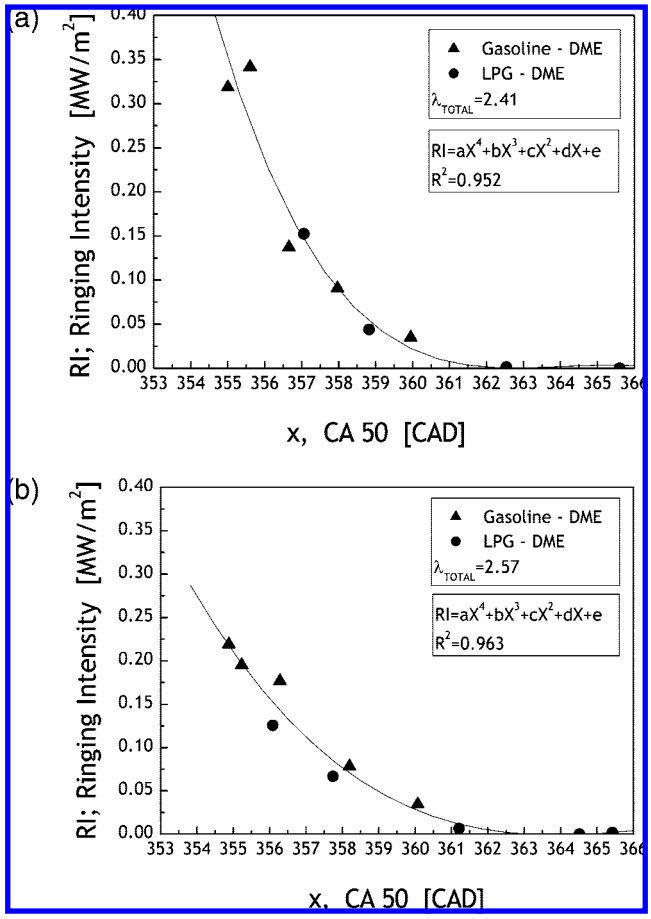

Figure 9. RI of HCCI combustion with respect to CA50 (crank angle degree at 50% mass fraction burned) at 1000 rpm: (a) $\lambda_{total} = 2.41$ and (b) $\lambda_{total} = 2.57$.

the emission of CO was minimized because of the maximized CO oxidation during the expansion stroke at a RI less than 0.5 MW/m^2 because of the high combustion temperature.

Another problem of HCCI emission is the HC emissions.[1] The main source of HC emission is the captured fuel in the crevice volume of the combustion chamber. To normalize the λ_{total} effect, the HC emission was divided by the exhaust emission, which contains carbon (CO, CO_2, and HC), using eq 3[2]

$$\text{percentage of unburned fuel flow} = \frac{\text{HC}}{\text{HC} + \text{CO} + \text{CO}_2} \quad (3)$$

where HC is HC emission, CO is CO emission, and CO_2 is CO_2 emission.

The HC emission ratio decreased as the RI increased, and it was approximately 35−39%. However, the percentage of unburned fuel flow was almost 47% at low RI conditions. It attributed to the high quenching effects because of low combustion temperature. The CO/CO_2 ratio and HC emission trends can be explained by the burn duration. Figure 11 shows the exhaust emissions with respect to λ_{total}. HC and CO_2 emissions were reduced as the λ_{total} was increased. CO emission was increased because of the reduced oxidation reaction and increased λ_{total}. Under all experimental conditions, NO_x emission can be negligible. Figure 12 shows the burn duration of the gasoline−DME and LPG−DME HCCI engines with respect to the RI. The RI is the index of knock intensity. However, the burn duration does not increase with the RI. The burn duration was approximately 2 CADs at higher RI values, >5 MW/m^3.

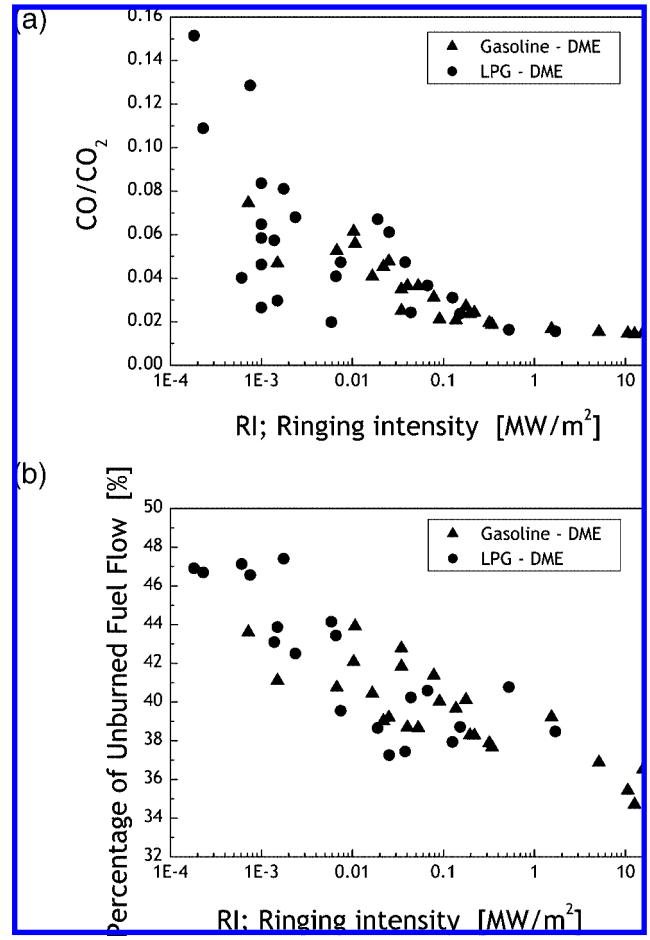

Figure 10. Exhaust emissions of HCCI combustion with respect to RI at 1000 rpm: (a) CO/CO_2 emission ratio and (b) HC emission (as percentages of the total carbon in the initial fuel charge).

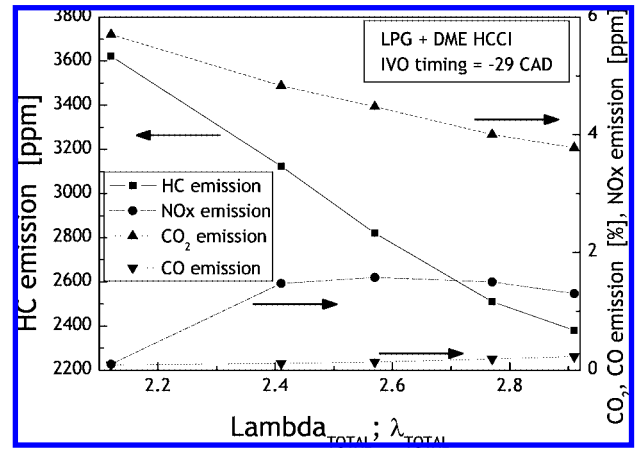

Figure 11. Exhaust emissions of LPG−DME HCCI combustion with respect to λ_{total} at 1000 rpm.

The reduced HC and CO emissions were the results of the high combustion temperature with short and vigorous combustion.

4. Conclusions

The effects of RI, combustion duration, and normalized exhaust emission characteristics in LPG−DME and gasoline−DME HCCI engines at different valve timings were investigated. Analysis of RI was performed to verify the HCCI combustion characteristics. The following conclusions were drawn from the experimental results.

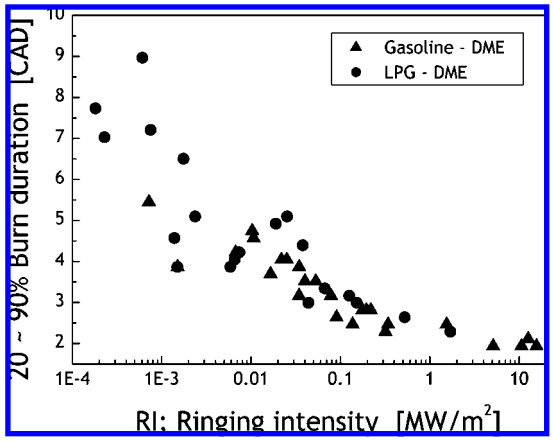

Figure 12. Burn duration of HCCI combustion with respect to RI at 1000 rpm.

The LPG−DME HCCI had a wider operating range than the gasoline−DME HCCI because of its higher octane number and higher latent heat of vaporization. The IMEP of the gasoline−DME and LPG−DME HCCI was significantly decreased when the λ_{total} is lower than 2.4. These IMEP losses at low λ_{total} regions are because of early combustion. The relationship between the IMEP and RI showed that the IMEP of the gasoline−DME and LPG−DME HCCI was decreased when the RI was over 0.5 MW/m^2. To reduce the RI, retarded IVO timing was an effective way by reducing the amount of intake charge density. The RI was higher than 0.5 MW/m^2, resulting from the P_{max} greater than 6.5 MPa. There were optimum fuel quantity and intake valve open timing for the best IMEP and lower RI. The RI can be estimated by the CA50 or P_{max}. The reduced HC and CO emissions were the results of the high combustion temperature with short and vigorous combustion.

Acknowledgment. The authors express their appreciation to the Combustion Engineering Research Center (CERC) of the Korea Advanced Institute of Science and Technology (KAIST) for the financial support.

Nomenclature

γ = specific heat ratio
λ = relative air/fuel ratio
N = number of cycles
P = cylinder combustion pressure
$(\partial p/\partial t)_{max}$ = maximum pressure rise
R = universal gas constant
T = temperature

Abbreviations
ATDC = after top dead center
BBDC = before bottom dead center
BTDC = before top dead center
CAD = crank angle degree
CO = carbon monoxide
CO_2 = carbon dioxide
DME = dimethyl ether
HC = hydrocarbon
HCCI = homogeneous charge compression ignition
IMEP = indicated mean effective pressure
IMPG = integral of modulus of pressure gradient
IMPO = integral of modulus of pressure oscillation
IVO = intake valve open
LHV = low heating value
LPG = liquefied petroleum gas
LTR = low-temperature reaction
MAPO = maximum amplitude of pressure oscillation
MFB = mass fraction burned
NO_x = nitric oxide
RI = ringing intensity
TDC = top dead center

EF800846U